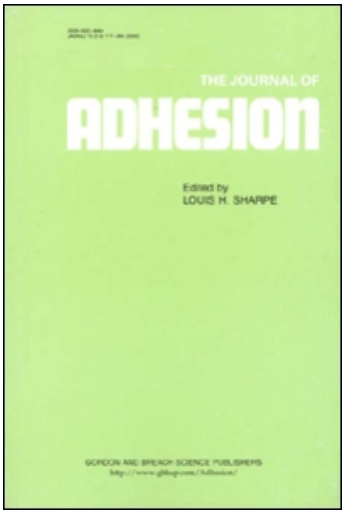

The Journal of Adhesion
Publication details, including instructions for authors and subscription information:
http://www.informaworld.com/smpp/title~content=t713453635

Peel Test Using Nonstationary Peel Method

Hiroyoshi Obori[a]; Mitsuru Takenaga[b]; Akira Nakamura[c]
[a] Product and Technology Department, Teraoka Seisakusho Co Ltd, Tokyo, Japan [b] Department of Materials Science, Faculty of Science and Engineering Science, University of Tokyo in Yamaguchi, Yamaguchi, Japan [c] Department of Applied physics, Faculty of Science, Science University of Tokyo, Tokyo, Japan

To cite this Article Obori, Hiroyoshi , Takenaga, Mitsuru and Nakamura, Akira(1996) 'Peel Test Using Nonstationary Peel Method', The Journal of Adhesion, 59: 1, 127 — 134
To link to this Article: DOI: 10.1080/00218469608011082
URL: http://dx.doi.org/10.1080/00218469608011082

J. Adhesion, 1996, Vol. 59, pp. 127–134
Reprints available directly from the publisher
Photocopying permitted by license only

Peel Test Using Nonstationary Peel Method*

HIROYOSHI OBORI**

Product and Technology Department, Teraoka Seisakusho Co., L td., 1-4-22 Hiromachi, Shinagawa, Tokyo 140, Japan

MITSURU TAKENAGA

Department of Materials Science, Faculty of Science and Engineering, Science University of Tokyo in Yamaguchi, 1-1-1 Daigaku-Dori, Onoda, Yamaguchi 756, Japan

and

AKIRA NAKAMURA

Department of Applied physics, Faculty of Science, Science University of Tokyo, 1-3 Kagurazaka, Shinjuku, Tokyo 161, Japan

(In final form January 19, 1996)

The cohesive peel spectra of pressure-sensitive adhesive (PSA) tapes have been measured using a nonstationary peel tester. The experimental evidence and a viscoelastic analysis based on a peel model indicate that there are no significant effects of acceleration in the normal rate region. The nonstationary peel tester can be regarded as a useful tool for testing and evaluating PSA tapes.

KEY WORDS: Peel spectra; peel model; pressure-seensitive adhesive tapes; viscoelastic analysis; peel acceleration effects; testing; evaluation.

INTRODUCTION

The nonstationary peel method has been applied to testing of the peel behavior for a variety of pressure-sensitive adhesive (PSA) tapes; this technique allows one to obtain the spread peel spectra from a cycle run of the accelerating and decelerating peels for short-length tapes.[1,2] This is useful for studies about the peel transition between cohesive and interfacial failures, including stick-slip behavior.

Conventional peel phenomena have been analyzed with a combined model of a three-element structure for the adhesive and an elastic beam for the backing.[3] The Voigt element[4,9] or the Maxwell element,[5,9] connected to backings deformed in a

* Presented at the International Adhension Symposium, *IAS'94 Japan*, at the 30th Anniversary Meeting of the Adhesion Society of Japan, Yokohama, Japan, November 6–10, 1994.

**Corresponding author.

curved shape, were also proposed. The results of model calculation gave an s-type curve, in agreement with those for measured peel curves.

In this paper, the peel behavior at low rates, measured using a nonstationary method, is interpreted with a viscoelastic model. This model, consisting of Maxwell elements with different relaxation times, is based on a prototype of the Hata model[8]. The good agreement between model analysis and experiment indicates the usefulness of this nonstationary method.

EXPERIMENTAL

A pressure-sensitive adhesive tape was prepared using a special adhesive made from a blend of masticated natural rubber (40%) and a tackifier (60%) consisting of the pentaerythritol ester of hydrogenated rosin. The thickness of the adhesive was 30 μm. The sample tape with backings of a 25 μm-thick PET film was cut into 10mm-wide strips. The surfaces of Pyrex® glass for the substrate were cleaned with the procedure previously described.[1] The tape adhered onto the substrate was kept for a day at ambient temperatures in an air-conditioned room to achieve steady state adhesion.

The peel measurement at a peel angle of 180° in a cycle of accelerating and decelerating peels was normally done at room temperature in air by use of a nonstationary peel tester. The details of the tester have been described elsewhere.[2] In the present measurement, three kinds of peel rate processes, called the stationary, constant accelerating, and variable accelerating peels, were utilized. The respective peel rates, V_p with respect to the time, t, or peel distance, D_p, are expressed by

$$V_p = \text{const.} \tag{1}$$

$$V_p = At \tag{2}$$

$$V_p \leftarrow = V_0 \exp(BD_p) \tag{3}$$

where A is the constant peel acceleration, V_0 is the initial rate at $D_p = 0$, and B is a constant. In the third process, the peel acceleration is given with $A_p = BV_p^2$, and its magnitude decrease as the rate is lowered; the measurable rate range in a single run is very wide. In the latter two, the corresponding deceleration peels are represented in the same functional form with different constants: *e.g.*, $A_p = -A_p$ and $B = -B$.

RESULTS AND DISCUSSION

Figure 1 shows peel spectra in a cycle of accelerating and decelarating peels, related to the third process of Eq. (3). The failure mode was cohesive over a relatively wide range of peel rates, but was visually interfacial on the high rate side, *via* the transition region of the failure mode. In addition, the stationary peel force, related to Eq. (1), was measured. The data overlapped the nonstationary curve within experimental precision.

For the same sample, the acceleration dependence in the low rate region was examined at various magnitudes of constant acceleration, related to Eq. (2). The resultant curves are dependent on the acceleration, as shown in Figure 2; the lower the peel rate, the stronger its dependency becomes. In each curve, a discontinuous change in peel spectra at a rate V_d was observed; below V_d the acceleration effect was dominant. We recognized from visual observation that at rates below V_d the adhesive only deforms, with no failure.

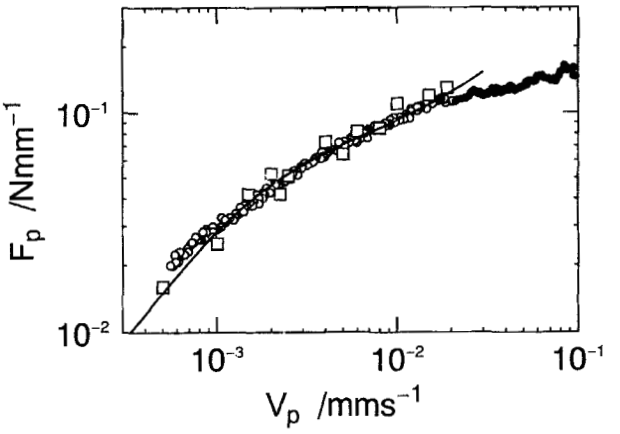

FIGURE 1 Peel force per tape width, F_p, against peel rate, V_p. Squares, in stationary peel; open circles, in decelerating peel with $B = -0.1$ mm^{-1}; solid curve, calculated from Eq. (5) with $\eta_1 = 6.3$[N^{-2}s], $\eta_2 = 0.63$[N^{-2}s], $\varepsilon_b = 70$, $\tau_1 = 420$[s]. Note that no data in accelerating peel have been plotted so as to avoid overlap, and that solid circles denote interfacial failure.

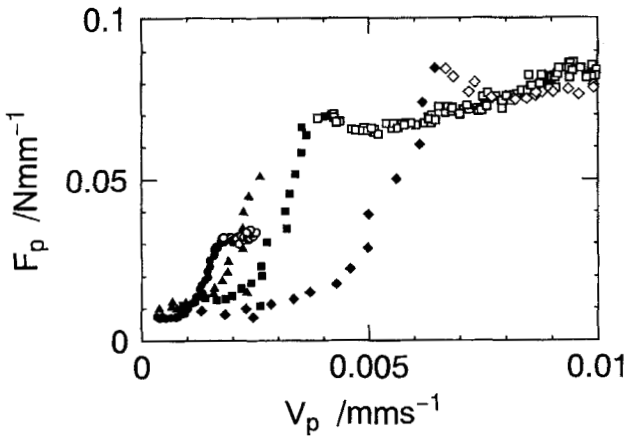

FIGURE 2 Peel force per tape width, F_p, against peel rate V_p, in constant acceleration peel: A_p [mm/s^2] $= 5.3 \times 10^{-7}$, (○); 2.4×10^{-6}, (△); 4.1×10^{-6}, (□); 1.7×10^{-5}, (◇). Open and solid symbols denote cohesive failure and the initial deformation prior to failure, respectively.

Viscoelastic Model

The peel behavior measured with this tester is interpreted by use of a viscoelastic model[8,9], consisting of Maxwell elements with relaxation times τ_j *i.e.*, the ratio of the viscosity, η_j, of the dashpot and the elastic modulus, G_j, of the spring, as Figure 3 shows in $j = 1, 2$. The relaxation time τ_1 is associated with the viscoelasticity of long-chain components in the pressure-sensitive adhesive, while τ_2 is associated with that of short-chain components. The relation $\tau_1 > \tau_2$ is effective in the normal range of strain rates. For cohesive failure peels in the low rate region, the contribution from τ_1 is more significant than that from the τ_2 component.

The cohesive failure criterion is defined as follows: the failure occurs when the total strain, $\varepsilon (= \varepsilon_1$ or ε_2: the respective values are the strains of the first and second Maxwell elements), has reached a critical strain, ε_b, and is constant; this is called the strain-controlled cohesive failure. In the present treatment, the elastic effect caused by backings will not be considered, because we focus on nonstationary behavior.

Figure 4 shows the schematic side-view peel profile. The adhesive adhered onto a substrate is divided into volume elements, each of which is numerated by $i = 1, 2 \ldots$ from the initial peel point. With peeling at the strain rate v ($v = at$: a is the constant acceleration and t is the time elapsed), the peel point moves toward the larger numbered elements, and the i-th element will arrive at the peel point during the time t_i. After that, the i-th element starts to deform at $v_i (= at_i)$, and it breaks after the time t_b at the rate $v (= v_i + at_b)$, where t_b is the time when ε of the i-th element, which had experienced $\varepsilon = 0$, $v = v_i$, and $t = t_i$, reached $\varepsilon = \varepsilon_b$. The resultant stress, σ_p, at the

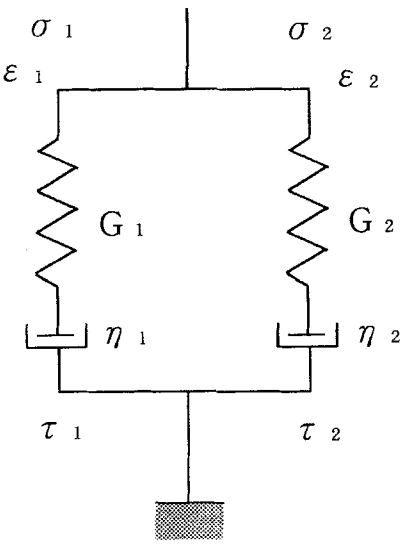

FIGURE 3 Viscoelastic model. Two Maxwell elements in parallel with each other: relaxation times, τ_j, elastic modulus of spring, G_j, viscosity of the dashpot, η_j, stresses, σ_j, and strains, ε_j ($j = 1,2$).

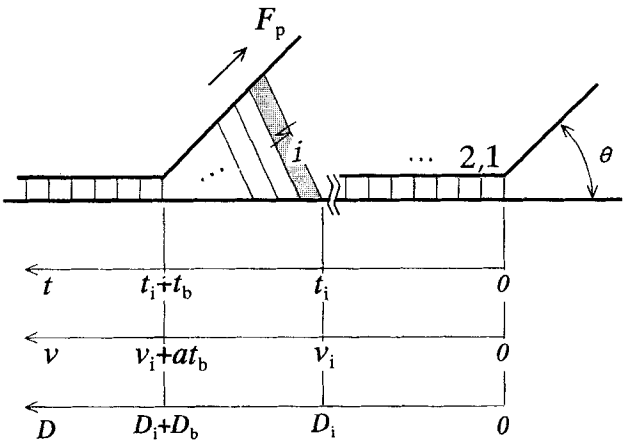

FIGURE 4 Schematic side-view profile of PSA tape peeling. The right is the initial state of pre-peeling. F_p is peel force, θ is peel angle, t is elapsed time, D_p is peel distance; see the text for other variables with subscript. The left is the peel state at the moment when the i-th volume element is just broken.

rate, v, or at the strain of $\varepsilon = \varepsilon_b = v_i t_b + (1/2)\, a t_b^2$, is expressed by

$$\sigma_p = \sum_{j=1}^{2} \eta_j \left[a t_b + (v_i - a\tau_j) \left\{ 1 - \exp\left(-\frac{t_b}{\tau_j} \right) \right\} \right] \tag{4}$$

If $a = 0$, then the stationary stress at v_i can be obtained as $\sigma_p = \Sigma \eta_j V_i \{1 - \exp(-t_b/\tau_j)\}$.

Before converting σ_p to the peel force, F_p, we consider a few necessary factors: As the cross-sectional area of the volume element decreases on deformation because of filamentation, we introduce the effective area ratio $R\,(= S/S_0)$ based on the volume constancy, where S anmd S_0 are the cross sections at ε and at no strain, respectively. The ratio R is readily represented as $R = 1/(1 + \varepsilon)$. Furthermore, the distance, D_b, from the peel point to the break element along the substrate can be obtained from $\varepsilon_b = 2D_b/gL_0$, by approximating an isosceles triangle to the deforming adhesive region, where L_0 is the adhesive thickness and g is the peel angle factor defined by $1/g = \sin(\theta/2)$ for the peel angle θ.

The peel force, F_p, is obtained by assuming no interaction among the divided elements and a uniform stress distribution for all the elements existing between the peel point and D_b. In the latter assumption, the stress of the related elements is the same as that at the distance D_b; but note that they have different forces owing to their R-dependent cross-sections. This is a rough approximation based on the experiment results from Kaelble.[6] Thus we obtain the peel force per tape width, F_p, with respect to the peel rate, V_p, corresponding to $v\,(= v_i + at_b)$, by summation of each force from the peel point to D_b:

$$F_p = \frac{1}{2} g^2 L_0 \ln(1 + \varepsilon_b)\, \sigma_p \tag{5}$$

where V and a, being implicitly involved in σ_p, are transformed by multiplying V_p and peel acceleration A_p. by the factor (1/2) gL_0. The stationary peel force can be obtained by substituting $a = 0$, and the force in the decelerating peel by reversing the sign of the acceleration.

In the accelerating peel of this test method, the initial deformation of the adhesive without failure is involved, as also shown experimentally; the force per tape width, F_d, for initial deformation at very low rates, if one makes the approximation $\exp(-t/\tau_2) = 0$, is approximated by

$$F_d = \frac{1}{2}g^2 L_0 \ln\left(1 + \frac{1}{2}at^2\right)\left[(\eta_1 + \eta_2)at - \eta_1\tau_1 a\left\{1 - \exp\left(-\frac{t}{\tau_1}\right)\right\}\right] \tag{6}$$

From the intersection of the curves of failure and deformation, expressed by Eqs. (5) and (6), respectively, a characteristic rate, V_d, at which adhesive failure occurs, is obtained to be $V_d = (gL_0\varepsilon_b A_p)^{1/2}$; in other words, using the test results of Figure 2, we can estimate the ε_b value from the plot of V_d^2 against A_p, if other parameter are known. Another derivation under the condition of $\varepsilon = \varepsilon_b$ at $t = t_b$, using $\varepsilon = (1/2)\, at^2$, $v = at$, $A_p = (1/2)\, gL_0$a, and $V_p = (1/2)\, gL_0 v$, also gives a similar relation for V_d.

Model Calculation

Figure 5 shows numerically calculated curves, using Eq. (5) for the stationary and decelerating peels, and Eqs. (5) and (6) for the accelerating peel, with appropriate values of $\eta_1 = 100$ Ns/mm^2, $\eta_2 = 10$ Ns/mm^2, $\tau_1 = 2000$s, $\tau_2 = 0.02$s, $L_0 = 30$ μm, $g = 1$ and $a = \pm 1 \times 10^{-4}$ mms^{-2}. In this calculation, the rate $v(= v_i + at_b)$ was divided into the constant interval of v_i and, further, the t_b time at any v_i was varied

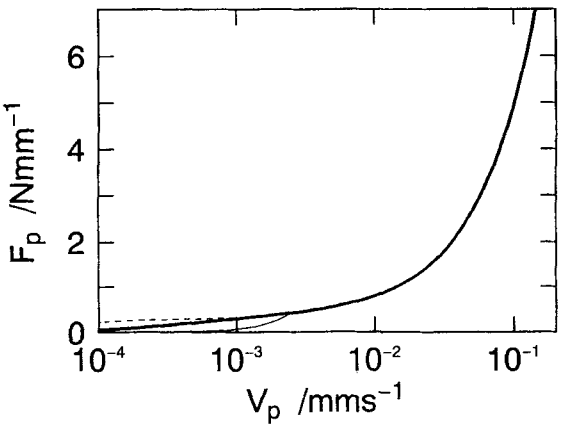

FIGURE 5 Peel force per tape width, F_p, calculated from Eq.(5) in stationary, accelerating and decelerating peels; $A_p = 0$, $\pm 5 \times 10^{-6}$ mm/s^2, $\eta_1 = 100$ Ns/mm^2, $\eta_2 = 10$ Ns/mm^2, $\tau_1 = 2000$ s, $\tau_2 = 0.02$ s, $L_0 = 30$ μm, $g = 1$. At low rates in accelerating peel, the deformation force, F_d, per tape width is calculated from Eq.(6). Dashed line, decelerating; bold solid line, stationary; narrow solid line, accelerating and initial deformation. Note that these lines overlap in the middle and high rate regions.

so as to satisfy $\varepsilon_b = v_i t_b + (1/2)\, a t_b^2 = 100$. In the medium and high rate regions, no appreciable differences between their curves was seen; but there is a much smaller degree of deviation depending on factors such as the relaxation time and the magnitudes of acceleration and rate. In the low rate region, the relatively large deviations of the accelerating curve, including the initial deformation, and of decelerating curves, were recognized; to examine the effect, the dependence of acceleration was tested in the spread range of deceleration and acceleration, *i.e.* $A_p = 0, \pm 2.5 \times 10^{-6}$, $\pm 5 \times 10^{-6}$, $\pm 1 \times 10^{-5}$ mm/s^2, if other constants were the same as above. As illustrated in Figure 6, the results shows that as a whole the larger the magnitude of A_p, the larger the deviation from the stationary curve becomes. It is expected that when the variable rate mode in this nonstationary method is used, such deviation is reduced because the magnitude of acceleration lowers with decrease in rate.

Comparison with Experimental Results

In the low peel rate region where V_p is smaller than a rate of $V_2 (= gL_0\varepsilon_b/2\tau_2)$, the stationary peel force is approximated by

$$F_p \sim C_1(\eta_1 + \eta_2) V_p \quad \text{at } V_p < V_1 \tag{7}$$

$$F_p \sim C_1 \eta_2 V_p + C_2 \quad \text{at } V_1 < V_p \tag{8}$$

where $C_1 = g \ln(1 + \varepsilon_b)$, $C_2 = C_1 \eta_1 V_1$, and $V_1 (= gL_0\varepsilon_b/2\tau_1) < V_2$, independent of the rate. Using Eqs. (7) and (8) and the stationary data, we estimate the effective values of η_1, η_2, τ_1 and G_1. Before that, a value of $\varepsilon_b = 70$ was estimated from the maximum strain of fibrils which has been just broken, using the observed results of a microscopic video. According to Eq. (7) and since $C_1 = 4.3$ as calculated, the initial slope gives $C_1(\eta_1 + \eta_2) = 27$ Ns/mm^2; since $\eta_1 \gg \eta_2$, $\eta_1 = 6.3$ Ns/mm^2. From comparison

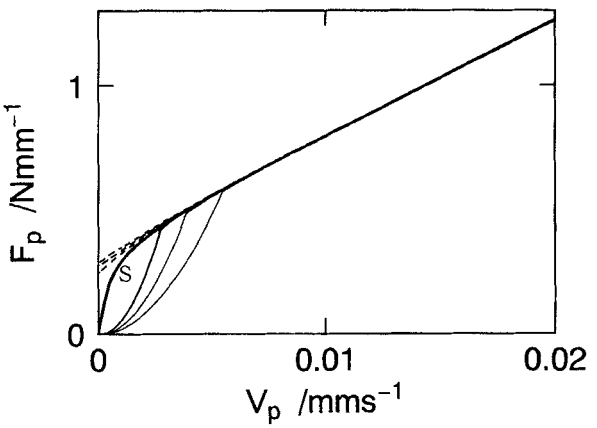

FIGURE 6 Peel force per tape width, F_p, in stationary, acclerating and decelerating peels as parameters of acceleration; A_p/mms$^{-2} = 0$; $\pm 2.5 \times 10^{-6}$; $\pm 5 \times 10^{-6}$; $\pm 1 \times 10^{-5}$ mm/s. Curve S denotes stationary peel; dashed lines, decelerating; solid lines, accelerating including the initial deformation at very low rates. Magnitudes of A_p become larger on proceeding upward or downward from curve S.

TABLE I
Values of parameters estimated from comparison with model calculation and test results

η_1[Ns/mm^2]	η_2[Ns/mm^2]	τ_1[s]	ε_b	V_1[mm/s]
6.3	0.63	420	70	0.0025

of the higher-rate data with Eq. (8), the fitted line had the slope of $C_1\eta_2 = 2.7$ Ns/mm^2 and the intercept of $C_2 = 0.068$ N/mm; thus, we gave $\eta_2 = 0.63$ Ns/mm^2 and $\tau_1 = 420$ s, leading to $G_1 = 0.015$ N/mm^2. These values are listed in Table I; the overall calculated curve is compared with the measured data, as exhibited in Figure 1.

From nonstationary data, an estimate of the relaxation time was also made using the relation $F_p \sim C_1\eta_1(V_p - \tau_1 A_p)$ at $V_p > A_p\tau_1$. In Figure 2, let us draw lines with the slope of $C_1\eta_1$ as fits to each set of data; and the plot of the rate, V_0, at $F_p = 0$ for each line against the corresponding acceleration, A_p, gives a straight line with the slope including the relaxation time of $\tau_1 = 500$ s, consistent with that from the stationary data. Furthermore, the relaxation measurement[7] of the similar adhesive has given a relaxation time of the same order as our values.

CONCLUSION

The peel force *vs.* peel rate characteristics, including the deformation process in the initial accelerating peel, were measured with a nonstationary peel tester. The peel spectra were analyzed using a viscoelastic peel model. The qualitative agreement between test results and model analysis indicated that in cohesive failure peeling, over the normal rate range, the degree of the acceleration effect was not significant and that the nonstationary peel technique could be regarded as a useful tool for testing and evaluating the peel spectra of PSA tapes.

References

1. H. Obori, M. Takenaga, and A. Kasai, *J. Appl. Polym. Sci.* **46**, 553 (1992).
2. H. Obori, M. Takenaga, A. Aniwar, and A. Nakamura, *J. Appl. Polym. Sci.* **53**, 993 (1994).
3. F.S.C. Chang, *Trans. Soc. Rheol.* **4**, 75 (1960).
4. T. Hata, *Materials* **13**, 341 (1964) (in Japanese).
5. K. Fukuzawa, *J. Adhesion Soc. Jpn.* **5**, 294 (1969) (in Japanese).
6. D.H. Kaelble, *Trans. Soc. Rheol.* **9**(2), 135 (1965).
7. K. Kamagata, H. Kosaka, K. Hino, and M. Toyama, *J. Appl. Polym. Sci.* **15** 483 (1971).
8. T. Hata, *J. Adhesion* **4**, 161 (1972).
9. H. Mizumachi, *J. Appl. Polym. Sci.* **30**, 2675 (1985).